Changes in bedload transport rate associated with episodic sediment supply in a Japanese headwater channel

Fumitoshi Imaizumi[a,*], Takashi Gomi[b], Sohei Kobayashi[c], and Junjiro N. Negishi[d]

[*]corresponding authour; [a] Graduate School of Life and Environmental Sciences, University of Tsukuba, Ikawa Experimental Forest, 1621-2, Ikawa, Aoi, Shizuoka, 428-0504 Japan

E-mail: imaizumi@sakura.cc.tsukuba.ac.jp

Tel: +81-54-260-2419; Fax: +81-54-260-2626

[b]Department of International Environmental and Agricultural Science, Tokyo University of Agriculture and Technology, 3-5-8 Saiwai-cho, Fuchu, Tokyo, 183-8509, Japan

Tel/Fax: +81-42-367-5751; E-mail: gomit@cc.tuat.ac.jp

[c]Incorporated Administrative Agency Public Works Research Institute, 1-6, Minamihara, Tsukuba, Ibaraki, 305-8516 Japan.

[d]Aqua Restoration Research Centre, Incorporated Administrative Agency Public Works Research Institute, Kawashima Kasada, Kakamigahara, Gifu, 501-6021 Japan.

Abstract

We conducted field monitoring of bedload transport rate associated with experimental sediment release in a natural channel to clarify behavior of the supplied sediment on mixed size bed. Observation of bedload rate at two sites along the 30 m channel reach revealed that downstream migration of finer particles delay compared with coarser particles. Ratio of the bedload sediment that deposited during the migration was higher for finer sediments. These behaviors of the mixed size particles were clear during passage of the sediment wave without changes in water discharge. Flashing peak of discharge that caused artificially by opening of the dam gate did not destroy channel bed structure including steps and pools formed by coarser sediments, and only small amount of bedload was mobilized. Both reach scale channel features including steps, pools, and riffles as well as fine scale features (i.e., armor coat) likely increased critical shear stress of particles and decreased bedload rate during our experiment. Extreme sediment supply induced two types of sediment deposition; (1) filling the pools in reach sales and (2) the intrusion of fine particles into the coarser sediment that formed an armour layer. The all grain size fractions can deposit as type (1) when shear stress of stream water is not enough to entrain bedload particles, while deposition type (2) occurs when finer sediment pass over channel bed on which armor coat is well-developed. Deposition of finer sediment into coarser sediment that forms armor coat is affected by grain size distribution of bed surface sediment. Thus, impact of the sediment supply on downstream channel depends on both bedforms and grain size distribution of bed surface sediment over which the supplied sediment pass.

Keywords: Gravel bed river; Bedload transport; Channel bed features; Sediment supply; Sediment flushing

Introduction

The sediment supply from hill slopes into channels is one of the most important factors affecting the bedload transport rate, especially in mountainous areas where the sediment reaches the channels directly (*e.g.*, Lisle *et al.*, 2001; Gomi and Sidle, 2003; Gomi *et al.*, 2004; Imaizumi and Sidle, 2007). Wide grain-size distributions of both the supplied materials and the available bed material sediments characterize the types of bedload entrainment and the transported grain sizes during storm events (*e.g.*, Bunte, 1992; Carling *et al.*, 1998; Lenzi *et al.*, 1999). The movement of the supplied sediment can typically be affected by localized roughness elements and the different types of channel morphology, including channel steps, pools, and riffles, which are formed along headwater channels (Ashida *et al.*, 1978b; Ashida *et al.*, 1979; Sidle, 1988; Lenzi, 2001). Depending on the sediment supply and the transport conditions, an armour layer can form on the bed surface, which promotes complex interactions between the incipient sediment movement and shear stress (*e.g.*, Dietrich *et al.*, 1989; Rosen, 1994; Montgomery and Buffington, 1997; Sidle, 1998; Emmett and Wolman, 2001). The mobility of the sediment differs among various grain-size fractions depending on the transport capacity and the sediment-supply conditions (Parker *et al.*, 1982; Kuhnle, 1992; Wilcock, 1992; Wilcock, 1997). Despite the great advances that have been made in our understanding of bedload movement, observing the complex interactions between sediment supplies and the mobility of the bedload remains difficult.

Changes in the size distribution and the flux of the bedload sediment associated with the sediment supply (*e.g.*, slope failures and bank erosion) have been observed in many catchments (*e.g.*, Montgomery *et al.*, 1999; Laronne *et al.*, 2001; Gomi and Sidle, 2003; Imaizumi and Sidle, 2007). Due to the episodic nature of some sediment-supply processes (*e.g.*, landslides and debris flows), the timing and amount of sediment supplied during specific storm events can vary. Consequently, the sediment that is available for movement varies temporally during storm events (Bunte, 1992; Komar and Shih, 1992; Cudden and Hoey, 2003; Imaizumi *et al.*, 2005). The bedload can be entrained selectively because of the variability of flow velocity and the presence of various channel roughness elements (*e.g.*, on the bed surface and at the channel reach scale), so the size distribution of the bedload is not identical to that of the substrate. Intensive field observations are essential to investigate the relationships between the bedload transport rate and the sediment supply. However, data regarding the temporal changes in bedload rate for various size fractions are scarce, because of the difficulty involved in conducting intensive observations during natural sediment-supply events. Flume studies, which are typically conducted to examine the influence of the sediment supply on the transport rate (*e.g.*, Lisle et al., 2001), are not suitable for reproducing natural channel conditions (*i.e.*, the bed form and grain-size distribution). Field experiments in natural rivers are therefore needed to understand the effects of the episodic sediment supply in natural gravel-bed rivers and the downstream movement of the released sediment in headwater channels.

The overall aim of the current study was to clarify the behaviour of the supplied sediment in headwater channels based on experimental sediment release. The specific objectives included observing changes in the bedload rate for various grain-size fractions during a sediment-supply event, and elucidating the influence of the grain-size distribution of the bed-surface material and the bed forms on the bedload rate. The results provide information on the sediment accumulation and sorting processes after episodic sediment release in gravel-bed rivers.

Study area

The study was conducted in the Hirudani experimental watershed (137°35′E; 36°16′N) operated by the Disaster Prevention Research Institute of Kyoto University, Japan. The Hirudani watershed, which has a drainage area of 0.85 km^2, is a headwater of the Zintsu River, located in central Japan (Figure 1). The elevation of the experimental watershed ranges from 1,165 m above sea level (a.s.l.) at the junction of the Ashiaraidani River — a tributary of the Zintsu River — at the western end of the watershed to 2,085 m a.s.l. at the south-eastern end of the watershed. The upper half of the watershed (> 1,600 m a.s.l.) mainly comprises Carboniferous and Permian slate, while the lower half is underlain by Mesozoic granite porphyry and quartz porphyry. Small landslides and exposed soils at the northern end of the watershed are the major sediment sources (Yano *et al.*, 1967). Freeze–thaw and subsequent dry ravel occur in early winter and late spring (Sawada, 1985). The average annual rainfall at the Hirudani experimental watershed is approximately 2,300 mm (Sawada, 1985), and snow accounts for 20% of the annual precipitation. The entire watershed is covered by snow (mean depth, > 50 cm on average) from December to March.

A check dam for measuring sediment transport and runoff was constructed on the Hirudani watershed in 1966, approximately 200 m upstream from the junction with the Ashiaraidani River (Yano *et al.*, 1967). Since then, a series of intensive field investigations has been conducted to gain insight into the bedload yields and the suspended sediment concentrations (SSCs; Ashida *et al.*, 1975; Sawada, 1985). The bedload sediment yield is usually identified during heavy rainfall events with peak discharges exceeding 0.05 m^3 s^{-1}; no sediment transport, including fine sediments, has been identified by bedload sampling below this critical discharge level (Ashida *et al.*, 1975; Ashida *et al.*, 1976). Snowmelt from April to the beginning of June causes sediment transport (Ashida *et al.*, 1975; Ashida *et al.*, 1976).

All of the bedload sediments from upstream were captured in the sediment pond behind the dam. The accumulated sediment in the pond was typically released once a year, in order to maintain the sediment-storage capacity of the dam. To release the sediment, the gate of the dam was opened. Both the water and the sediment were flushed out of the dam simultaneously. The released sediment moved downstream after the first pulse of flushing. The channel reach of the section downstream from the dam was suitable for observing the sediment wave migration and the channel adjustment after sediment release. Several hours after the first flushing (typically 3 h after the opening of the gate), the gate was closed again for the second flushing.

The channel gradient of the downstream section (from site A to the junction) was approximately 15.8%, and the channel gradient in the upper reach of the downstream segment (*e.g.*, sites A and B) was 14.6%, which was within the usual gradient range for step-pool sequences (Rosen, 1994; Montgomery and Buffington, 1997). Three steps and pools were identified in the section from site A to site B by field surveys (Figure 2). Riffles were the most dominant bed form in this section. There was a paved road (3 m in width) between the dam and site A, and a culvert (1 m in diameter) crossed under the road. To avoid the culvert effect on bedload rate, the study area was at least 10 m downstream of the culvert outlet.

Methodology

Field experiments and measurements

The sediment-supply experiment was conducted on June 17, 2005. As the Hirudani watershed had not experienced heavy rainfall (total rainfall, > 10 mm) since June 5, 2005, the flow discharge remained stable (the base-flow condition) before the experiment. The gate of the dam was opened at 11:02 for the first flushing, and the deposits in the dam pond were evacuated by impounded water flowing out from the gate. We also scooped out the sediment soon after the opening of the gate, to accelerate the evacuation of the sediment from the dam. The gate was closed at 11:55 in order to retain water for the second flushing.

The bedload sediment was sampled using Helley-Smith samplers (76 mm intake) at sites A and B (Figure 1). The sampling interval was approximately 1–2 min directly after the dam opening, and was extended up to 5 min at 11:30 when the discharge volume tapered down (the steady-state condition). The bedload rate of the Helley-Smith samplers was calculated as the dry weight of the sampled sediment divided by the duration of the sampling events (average duration, 30 s). The bedload sampling was paused at 13:10, prior to the second flushing. The bedload rate was multiplied by the ratio between the channel width, which changed over time, and the width of the sampler (76 mm), in order to estimate the bedload flux for the entire channel width. The grain-size distribution was analyzed using sieves with mesh sizes of 1, 2, 4, 8 and 16 mm. The efficiency of the 76-mm Helley-Smith sampler decreases as the grain size increases, especially at sizes larger than 16 mm (*e.g.*, Emmet, 1980; Vericat et al., 2006). Therefore, we did not analyze the bedload rate for particles larger than 16 mm. We assumed that the bedload sediment consisted of particles that were larger than fine sand (> 1 mm in diameter), because particles smaller than 1 mm were likely to be carried in suspension due to the rough and turbulent flow conditions in steep channels. Indeed, grab-water samples, which were intended to collect the suspended sediment, contained only sediments finer than 1 mm. The bedload was also sampled at site H_1 by a bedload trap consisting of a metal rectangular frame with a width of 40 cm, and a net (with an opening of about 1 mm) that covered the frame and captured the passing sediment. The trap was installed in the channel bed for the period between 15:00 on June 16 and 9:00 on June 17, to observe the bedload rate from the area upstream of the dam.

The water height was measured using a capacitance water-level probe (Trutrack, WT-HR) with a measurement range of 0.5 m (accuracy, ± 5 mm) at intervals of 30 s. Temporal changes in the cross-sectional area of the stream water were estimated from the water height recorded with the water-level probe and the cross-sectional surveys (Figure 2). The discharge was calculated from the cross-sectional area of the stream water based on the water velocity estimated using Manning's equation. The roughness coefficient of Manning's equation (0.08) was estimated from the channel gradient around site H_2 and the water velocity was measured using floats. As the deposition of bedload sediment might affect the roughness of the channel bed surface, the roughness coefficient might vary with time. However, we fixed the value of the Manning's roughness coefficient because of the difficulty in observing these temporal changes. Furthermore, the flow velocity observed using the floats represented the value near the water surface rather than the average value. Consequently, our estimation of flow velocity might have included some errors.

Three samples of the bed surface and subsurface material (depth, < 10 cm) around site H_2 were collected before and after the sediment supply, to clarify the changes in the grain-size distribution of riffles. Each sample was shovelled into a scoop, to minimize the washing of fine sediments by stream flow. Because riffles occupied more than 70% of the area between sites A and B (Figure 2), we assumed that changes in the grain-size distribution around H_2 represented changes in the size distribution over the majority of the channel area. Three sediment samples were collected from the dam pond at various depths. The grain-size distribution of the deposited sediment in the dam pond was analyzed using the same sieve classes as those used for the bedload sediment. A detailed longitudinal profile of the channel reach was produced using an engineering level before the first flushing. A metal rod with a length of about 1 m was plunged into the bottom of a pool located about 5 m downstream of site A, in order to observe the difference in the bed-surface level before and after the experiment.

Analytical methods

Shear stress is one of the most important factors controlling the mobility of sediment. The dimensionless shear stress, τ_* (Shields parameter), which is an index used to compare shear stress values under different site conditions, is given by the following equation,

$$\tau^* = \tau\left((\sigma - \rho)gd\right)^{-1}, \qquad [1]$$

where σ is the mass density of the sediment (~2.65 kg m^{-3}), ρ is the mass density of water (~1.0 × 10^{3} kg m^{-3}), g is the acceleration of gravity (9.8 m s^{-2}), d is the grain size of the sediment (m), and τ is the shear stress (ρgRI, where R is the hydraulic radius (m) and I is the channel gradient).

Since it was first proposed by Parker *et al.* (1982), the fractional transport rate of bed materials has been applied to examine the size-dependent sediment mobility. The fractional transport rate (q_{bi}/F_{bi}), which is the transport rate of the individual size fractions (q_{bi}) divided by the proportion of each fraction (F_{bi}) in the bed material of the ith size range, is an effective indicator of the extent of selective mobility (Parker *et al.*, 1982; Wilcock and McArdell, 1993). The fractional transport rate of the transported sediment was calculated using the grain-size distributions of bedload samples collected at sites A and B. The bed-surface material collected at site H_2 was used to provide representative values for the bed surface and subsurface sediment. For the estimation of the fractional transport rate, we assumed that the particle-size distribution of the bed-surface sediment was constant during the bedload sampling period.

Results

Flushing water and changes in discharge

The discharge at site H_2 increased soon after the opening of the dam gate (Figure 3), and decreased gradually with some surges after the peak at 11:04 (0.15 m^{3} s^{-1}). The discharge had subsided to a level similar to that observed prior to the experiment by 11:30, and thereafter remained at pre-flushing levels (Figure 3). We did not record discharge data after 12:04, because the aggradations around site H_2 prevented the water-level probe from functioning properly. No clear changes in discharge were observed after the cessation of bedload sampling. The changes in flow velocity and shear stress at sites A and B were estimated from the cross-sectional profile at each site and the discharge observed at site H_2 (Figure 3). Both the velocity and the shear stress peaked soon after the opening of the dam gate. The shear stress at site B exceeded that at site A, because of the steeper channel gradient. A culvert pipe located between the dam and site A might have affected the flow conditions (*i.e.*, the velocity and water height) immediately downstream of the pipe. Based on a field survey, no direct influence of the pipe on the flow around site A (*e.g.*, the jet from the pipe) was identified during the study period. We therefore believe that the direct impact of the pipe on the flow conditions in the channel between sites A and B was negligible.

Grab-water samples collected at intervals of 2–5 min until the dam gate was closed at 11:55 showed that the SSC ranged from 400 to 5,000 mg l^{-1}. The SSC during the first flushing ranged from 1,600 to 2,000 mg l^{-1}. Therefore, the suspended sediment did not significantly affect the density of the stream water during the experimental. Based on the field survey, the stream flow was characterized as Newtonian throughout the experimental period.

Grain-size distribution, bedload movement and channel morphology

Most of the released sediment was deposited immediately below the dam, which was located upstream of the culvert. Part of the sediment was transported further downstream, passing through the culvert and reaching site A. The sediment in the dam was finer than the bed-surface material around site H_2 before flushing (Figure 4). The bed-surface material around site H_2 became finer during the experiment because of the deposits from the dam. However, our post-flushing substrate sampling was conducted after the second flushing at 13:15. Therefore, the substrate size distribution after the experiment represented the sediment deposition associated with both the first and the second flushings.

The transported sediment tended to accumulate in the bed substrate during the passing of the sediment wave. The observation of the bed-surface level using a metal rod installed in the pool about 5 m downstream of site A indicated that 17.7 cm of sediment was deposited. The deposition of sediment was identified not only in pools but also in riffles. The total masses of the bedload sediment that passed the sampling sites were estimated as the sum of the bedload rate multiplied by the sampling interval (Table 2). The total mass of the bedload sediment was 691 and 201 kg at sites A and B, respectively. Therefore, a total of 490 kg sediment was deposited in the area between sites A and B, based on the mass-balance calculation. As the distance between sites A and B was 31.2 m, and the average channel width was 1 m, the mean amount of sediment that was deposited in the study reach was of 16 kg m^{-2}. Thus, the mean depth of deposition was approximately 8.5 mm, as calculated from a sediment density of 2.65 t m^{-3} and a porosity of 0.7. Sediment deposits that were > 10 cm in depth were identified in a pool, suggesting that their depth varied spatially in association with the channel topography. Based on the bedload samples, a total of 6.5 kg coarse sediment (> 16 mm) passed site A during the sampling period. No sediment coarser than 16 mm was sampled at site B. Even though the efficiency of the Helley-Smith sampler decreases drastically as the grain size increases (Emmet, 1980; Vericat et al., 2006), the relatively small amount of coarser bedload sediment compared with the total bedload weight (691 and 201 kg at sites A and B, respectively) implied that the coarser sediment constituted a small portion of the total bedload during the sampling period.

The channel morphology did not differ considerably before and after flushing. The step structures consisting of large boulders remained in the same locations after flushing. Therefore, the flush flooding and the sediment wave passing through the channel did not modify the channel reach morphology.

Bedload transport rate

The discharge before the experiment (0.048 m^3 s^{-1}) was slightly lower than the critical discharge for the initiation of bedload entrainment (0.05 m^3 s^{-1}) calculated from observations conducted during natural rainfall events in the Hirudani watershed (Ashida *et al.*, 1975; Ashida *et al.*, 1976). No bedload sediment, including fine sediments, was captured at site A or site B by the Helley-Smith samplers prior to the experimental flushing. There was no bedload transport of finer particles, including sediments with critical shear stress values lower than the shear stress before the experiment, which indicated that the channel bed was armoured before the experiment. The shear stress values before the dam opening were 85 and 140 N m^{-2} at sites A and B, respectively. A small bedload rate peak was observed at both sites within 1 min after the dam opening at 11:05. The peak discharge after the dam opening (0.155 m^3 s^{-1}) exceeded the critical discharge during natural rainfall events (0.05 m^3 s^{-1}). At this peak value, the transported bedload sediment at site B was tenfold greater than that at site A (0.208 kg s^{-1} and 0.024 kg s^{-1}, respectively; Figure 3). The maximum shear stress values during this flushing peak were 141 and 254 N m^{-2} at sites A and B, respectively. The bedload rate decreased rapidly after the peak discharge. The bedload transport rates at 11:06 at sites A and B were < 0.01 kg s^{-1}. The bedload rate began to increase at around 11:55 at site A, and the peak bedload transport rate (0.864 kg s^{-1} for all grain sizes) was recorded at 12:23. No clear change in the bedload rate occurred until 12:31 at site B. The bedload transport rate at site B peaked at 12:40 with a value of 0.232 kg s^{-1} for all grain sizes, and decreased gradually until the end of the observation period at 13:10. The bedload mass sampled at site H_1 from 15:00 on June 16 to 9:00 on June 17 was only 4.4 g (average bedload rate, 1×10^{-4} g s^{-1}). Thus, the bedload transport upstream of the dam was considered to be negligible with respect to the amount of sediment flushed from the dam.

The peak bedload rate for the coarser sediment was reached slightly faster than that for the finer sediment at both sampling sites (Table 1). The time lags between the peak bedload rates of the 1–2 mm sediments and the 8–16 mm sediments were 5 and 8 min at sites A and B, respectively. The highest peak bedload transport rate was observed for grain sizes ranging from 1 to 4 mm at site A. Finer sediments (*i.e.*, diameter, 1–4 mm) showed a sharp bedload peak compared with coarser sediments (*i.e.*, diameter, 8–16 mm). For all grain-size fractions, the total bedload transport rate at site B was smaller than that at site A (Table 2), indicating that sediments of all grain-size fractions were deposited in the area between sites A and B. The ratio of deposition was greatest (80%) for the 1–2 mm grain-size class, followed by the 2–4 mm grain-size class. The differences in the deposition ratio among the grain-size classes indicated significant sorting of the bedload material in the channel between sites A and B.

The bedload velocity, which was estimated as the time lag of the peak bedload rate between sites A and B divided by the distance between the two sites, ranged between 0.021 and 0.031 m s^{-1} (mean, 0.025 m s^{-1}; Table 1). The frontal part of the sediment wave might have been deposited within the area before reaching site B. Hence, the velocity might not precisely represent that of individual particles. Instead, the velocity can be considered as an index of the velocity of the sediment wave.

Fractional transport rate and dimensionless shear stress

The fractional transport rate was calculated for the small bedload rate peak immediately after the opening of the dam gate (11:04 to 11:05) and during the maximum bedload peak (at 12:23 for site A and at 12:40 for site B). For both of these peak bedload rates, the fractional transport rate of the finer sediment tended to exceed that of the coarser sediment (Figure 5). For the small bedload peaks at 11:04 and 11:05, the curves showed gradual decreases in the transport rate with increasing grain size. This showed that the sediment entrainment of the fine materials tended to be greater than that of the coarse materials.

Our observations indicated that most of the mobile sediments during the second peak originated from the sediment sources of the dam (the sediment wave). The fractional transport rate in the second sediment peak was approximately one to two orders of magnitude greater than that in the first sediment peak (during the peak flow) at site A. The ratio of the second sediment peak to the first sediment peak was the highest (53) for the 2–4 mm grain-size class and lowest (4.5) for the 8–4 mm grain-size class. The fractional transport ratio at site A decreased gradually with increasing grain size (Figure 5). By contrast, the ratio of the second sediment peak to the first sediment peak was < 3 in all grain-size classes at site B. The curve at site B showed a break in the slope where the transport rate began to decline with increasing grain size (d_i/d_{50}, 0.15). As the fractional transport rate between sites A and B was greatly diminished, significant selective deposition occurred in the 1–4 mm grain-size class under transport-limited conditions.

Discussion

Bedload transport and sediment accumulation

The transport rate of each grain-size fraction at sites A and B suggested significant sorting of bedload material and deposition in a relatively short 30-m channel reach (Table 2). An analysis of the fractional transport rate also showed that sediment with a diameter of 1–4 mm tended to be deposited in the channel reach (Figure 5). These results indicate that sediment deposition at the bed-surface scale roughness element including the matrix of the coarser sediment. This type of sediment deposition occurs when finer sediments pass over a channel bed with a well-developed armour layer. As finer sediment can clog the matrix of the armour layer, it was indeed selectively deposited during the experiment, leading to a greater deposition rate for fine particles (Table 2). The decreasing grain size of the bed-surface sediment during the experiment also indicated that the finer sediment settled into the matrix of the coarser sediment, as reported in previous studies (Ashida *et al.*, 1978a; Carling *et al.*, 1998, Lisle and Hilton, 1999; Figure 4).

Sediment also tended to accumulate in reach-scale channel roughness components (*i.e.*, pools) in the step-pool dominant channel reach. As the channel gradients did not differ significantly between sites A and B (Figure 2), the average cross-sectional shear stress was expected to be similar throughout the study section when the discharge was constant. Therefore, deposition was likely to have occurred in the pools where the flow velocity tended to be low. In fact, sediment deposition with a depth > 10 cm was observed in pools during our field survey. Sediment deposits in pools were noted during natural rainfall-runoff events according to field measurements conducted before and after natural rainfall events in the Hirudani watershed (Ashida *et al.*, 1978b; Ashida *et al.*, 1979; Ashida *et al.*, 1980; Fujita *et al*., 2005) and the other catchments (Lisle and Hilton, 1999; Lenzi, 2001).

With the exception of during the period when the sediment wave was passing, the changes in elevation and grain-size distribution of the bed-surface material might not have been significant during our experiment, as only a little bedload rate was observed. However, the deposition of bedload sediment during the passage of the sediment wave might have changed the channel conditions (*i.e.*, the elevation and grain-size distribution of the bed-surface material). These changes might have affected the hydraulic conditions as well as the amount of available material for subsequent bedload transport (Lisle and Hilton, 1999; Cudden and Hoey, 2003).

There were several possible sources of error associated with our sampling schemes and experimental flushing approach for evaluating bedload transport and deposition. The second flushing was conducted at 13:15, before the surface material at site H_2 was sampled to evaluate the effect of flushing on the bed-surface materials. Therefore, we were unable to examine the depositional conditions and the sediment accumulation in the armoured substrate layers that were exclusively related to the first flushing. Potential artefacts of bedload sampling might be associated with the use of a Helley-Smith bedload sampler. The effectiveness of sampling might differ among bedload fractions due to the relatively narrow intake compared with the channel width and the short sampling interval (Bunte *et al.*, 2004). The Helley-Smith sampler underestimates the bedload rate, especially in the larger grain-size range (e.g., Emmet, 1980; Vericat et al., 2006). Therefore, the sampling of large particles is likely to involve relatively large errors. Nevertheless, the sediment accumulation in pools and the changes in particle-size distributions in the bed subsurface showed that there were two types of deposition (*i.e.*, deposition at the bed-surface scale and in reach-scale roughness elements) in the area between sites A and B.

Bedload transport during flushing-discharge peak

The bedload transport observed immediately after the dam opening was induced by the increase in discharge under supply-limited conditions. Sediment for entrainment was available only from the bed surface and subsurface. As the bedload rate of the coarser sediment (*i.e.*, > 16 mm) comprising the armour layer and step pool was negligible, most of these structures remained stable during the flushing peak. The fine sediments in the bed-surface patches might be a source for bedload transport during the flushing peak (Garcia *et al*., 1999; Garcia *et al*., 2000; Laronne *et al*., 2001; Gibbins *et al.*, 2007).

Observations of bedload transport during natural rainfall events revealed that the grain-size distribution of the bedload sediment approached equal mobility conditions when the discharge exceeded 0.15 $m^3 s^{-1}$ (Ashida *et al.*, 1972; Ashida *et al.*, 1973; Ashida *et al.*, 1979). A significant amount of the bedload can be transported during such storm events, partly because of the destruction of the armour layer. In our experimental flushing, the maximum discharge observed at site H_2 was < 0.15 $m^3 s^{-1}$. Although the shear stress during the flushing peak (*e.g.*, τ^*_{50} = 0.23 at site A) exceeded the τ^*_{c50}, which usually ranges between 0.05 and 0.09 (Parker *et al.*, 1982; Andrews, 1983; Ferguson, 1994), transported large particles (*i.e.*, diameter, > d_{50}) were not observed during our experiment. Similarly high values of τ^*_{50} (0.14–0.20) with respect to the transported particles were also identified in other gravel-bed and boulder-bed rivers (Batalla and Martín-Vide, 2001; Lenzi *et al.*, 2006). While the armour layer is present, the bedload transport rate is potentially affected by the grain-size distribution of the bed surface, including the size distribution of the fine sediments in patches between the coarser particles (Laronne *et al*., 2001), rather than that of the subsurface. Once the armour layer has been destroyed, the grain-size distribution of the subsurface layer might also become an important factor for explaining the bedload transport rate.

Movement of sediment wave

The bedload transport after 11:55 was apparently caused by the arrival of the sediment wave from the dam, as changes in the bedload rate were not associated with the increase in discharge that is needed for re-migration of the bed material (Figure 3). As was the case with the bedload transport during the flushing peak after dam opening, selective transport was the dominant mode of bedload transport during the passage of the sediment wave, as shown by the analysis of the fractional transport rate (Figure 5). The velocity of stream water observed around site H_2 was about 0.5–1 m s^{-1} (Figure 2), indicating that the velocity of the sediment wave (0.021–0.031 m s^{-1}; Table 1) was an order of magnitude lower than that of the stream water. Under low-flow conditions, the bedload particles were deposited continuously and then transported through the channel reach along with the sediment wave (Lisle *et al.*, 2001).

Although the discharge remained in a steady state after 11:15, changes in the bedload rate were observed with the passage of the sediment wave. This indicated that the relationship between the bedload rate and shear stress was unclear during the passage of the sediment wave. A weak relationship between the bedload rate and shear stress has also been reported in other studies (Garcia *et al.*, 1999; Garcia *et al.*, 2000). The shear stress during the passage of the sediment wave (85 and 140 N m^{-2} at sites A and B, respectively) was lower than that during the flushing peak (142 and 218 N m^{-2}, respectively). However, more sediment particles tended to be mobilized when the sediment wave approached sites A and B. The sediment mobility for a given grain size is affected by the transport of sediment of other grain sizes (Andrews, 1983; Bunte, 1992; Batalla and Martín-Vide, 2001). As the critical shear stress for each grain-size class can be estimated based on the mean grain-size distribution (Andrews, 1983; Batalla and Martín-Vide, 2001), changes in the mean grain size associated with the sediment supply affect the indices of mobility of the bedload sediment for a given size classes. In addition, the deposition of fine particles in the matrix of coarse sediment decreases the protrusion of coarse particles on the channel bed. The critical shear stress decreases as the protrusion decreases (Carling, 1983), so the arrival of the sediment wave changes the critical shear stress of the coarse bed-surface sediment. As with the dimensionless shear stress for d_{50} in the flushing peak, the dimension shear stress during the arrival of the sediment wave (0.13 and 0.22 at site A and B, respectively) tended to exceed the τ^{*}_{c50} values reported in other catchments (usually ranging between 0.05 and 0.09; Parker *et al.*, 1982; Andrews, 1983; Ferguson, 1994). Despite such reported values, the maximum particle size of the bedload (< 31.5 mm) during the arrival of the sediment wave was smaller than the median diameter of the bed-surface material. In addition to the wide grain-size distribution of the bed material and the roughness elements provided by step-pool structures, the differences between the estimated critical shear stress and the transported materials probably enhanced the selective transport in the Hirudani watershed.

The peak bedload rate of the coarser sediments was reached before that of the finer sediments at both sites A and B (Table 1). Earlier occurrences of the coarser sediment peak than the finer sediment peak were also reported in other field observations and flume experiments (Ashida *et al.*, 1978a;

Imaizumi *et al.*, 2005). Differences in the timing of reaching the peak bedload transport rate of various grain-size fractions might be associated with the bed-surface roughness relative to the size of the transported sediment. For example, Ashida *et al.* (1978a) noted in a flume experiment that fine particles dropped into the matrix of the bed-surface material and/or the matrix of moving coarser particles. The matrix of coarse sediment on the bed surface (the armoured layers) needed to be buried in order to create a relatively smooth surface before the fine particles migrated further downstream. This resulted in delayed responses of fine particles relative to coarse particles.

Summary and Conclusions

We examined the bedload transport during experimental sediment release from a check dam in a headwater stream in Japan. Two types of bedload rate peak depending on different sediment-supply conditions were observed during the experiment: first, the transport of bed-surface sediment (*i.e.*, fine sediment in patches between coarse sediments) caused by the increase in discharge under supply-limited conditions; and second, the arrival of the sediment wave from the dam pond. Although the shear stress during the passage of the sediment wave was lower than that during the flushing peak, more sediment tended to be mobilized when the sediment wave approached. The experiment was conducted under low-discharge conditions, and the armour and step-pool structures remained stable during the experiment. However, the difference in the total volume of the bedload sediment between the two observation sites along the channel indicated that the deposition of sediment occurs as the sediment wave progresses downstream. Field observations revealed sediment deposition in pools as well as the intrusion of fine particles into the coarser sediment that formed an armour layer. Thus, the sediment supplies during a low-discharge event can significantly change both the bed-surface scale and the reach-scale channel structures. The impact of the sediment supply on the downstream channel depends on both the bed form and the grain-size distribution of the bed-surface sediment over which the supplied sediment passes. The water depth and the grain size of the substrate sediment, which control the shear stress, can be altered by changes in sediment availability during flushing and sediment wave migration.

In gravel-bed rivers, the impact of the sediment supply on the bedload rate has rarely been examined because of the difficulties involved in observing the bedload rate during natural rainfall events. As with the fine sediment found in patches between coarse particles (Garcia *et al*., 1999; Garcia *et al*., 2000; Laronne *et al*., 2001; Gibbins *et al.*, 2007), the sediment supply from a hill slope is an important factor that determines the bedload rate. Our study showed that changes in the sediment supply and associated changes in the bed-surface conditions controlled the mode of sediment transport with respect to the relative discharge and bedload rate. The short-term impact of episodic sediment supply (*i.e.*, landslides and debris flows) on the bedload rate in natural watersheds can be inferred from the findings of this study. The deposition of sediment in pools and substrates affects the habitat conditions for benthic macroinvertebrates and fish (Hartman *et al.*, 1996, Gomi *et al.*, 2002; Miller *et al.*, 2003; Geertsema and Pojar, 2007). In addition, changes in the microhydraulic conditions on the bed surface might influence the colonization patterns of drifting organisms. Further investigations are necessary to understand fully the effects of an extreme sediment supply on sediment transport in relation to the biological processes in headwater systems.

Acknowledgements

We thank Drs. Toyoaki Sawada, Masaharu Fujita, Daizo Tsutsumi and Yasuyuki Tada for help with the experiment. Thanks are also due to the staff of Kyoto University, Japan, for their support during the study. We are also grateful to Dr. Roy C. Sidle for assistance with our research grant and for providing survey tools for the experiment.

References

Andrews, E.D., 1983. Entrainment of gravel from naturally sorted riverbed material. *Geological Society of America Bulletin* 94: 1225–1231.

Ashida, K., Takahashi T., Mizuyama, T., 1978a. Study on bedload equations for mountain streams. *Journal of the Japan Society of Erosion Control Engineering* 107: 9–17 (In Japanese with English abstract).

Ashida, K., Takahashi, T., Okumura, T., Michiue, M., Sawada, T., 1972. Runoff processes, sediment yield and transport in a mountain watershed—some observations by Hodaka Sediment Observatory. *Annals of Disaster Prevention Research Institute*, *Kyoto University* 15B: 349–361 (in Japanese with English abstract).

Ashida, K., Takahashi, T., Sawada, T., 1973. Runoff processes, sediment yield and transport in a mountain watershed (2)—some observations by Hodaka Sediment Observatory. *Annals of Disaster Prevention Research Institute*, *Kyoto University* 16B: 401–409 (in Japanese with English abstract).

Ashida, K., Takahashi, T., Sawada, T., 1975. Runoff processes, sediment yield and transport in a mountain watershed (4)—some observations by Hodaka Sediment Observatory. *Annals of Disaster Prevention Research Institute*, *Kyoto University* 18B: 529–540 (in Japanese with English abstract).

Ashida, K., Takahashi, T., Sawada, T., 1976. Runoff processes, sediment yield and transport in a mountain watershed (5)—some observations by Hodaka Sediment Observatory. *Annals of Disaster Prevention Research Institute*, *Kyoto University* 19B: 345–360 (in Japanese with English abstract).

Ashida, K., Takahashi, T., Sawada, T., 1978b. Runoff processes, sediment yield and transport in a mountain watershed (7). *Annals of Disaster Prevention Research Institute*, *Kyoto University* 21B: 467–483 (in Japanese with English abstract).

Ashida, K., Takahashi, T., Sawada, T., 1979. Runoff processes, sediment yield and transport in a mountain watershed (8). *Annals of Disaster Prevention Research Institute*, *Kyoto University* 22B: 301–314 (in Japanese with English abstract).

Ashida, K., Takahashi, T., Sawada, T., 1980. Runoff processes, sediment yield and transport in a mountain watershed (9). *Annals of Disaster Prevention Research Institute*, *Kyoto University* 23B: 393–412 (in Japanese with English abstract).

Batalla, R.J., Martín-Vide J.P., 2001. Thresholds of particle entrainment in a poorly sorted sandy gravel-bed river. *Catena* 44: 223–243. DOI:10.1016/S0341-8162(00)00157-0.

Bunte, K., 1992. Particle number grain-size composition of bedload in a mountain stream. In: P. Billi, R.D. Hey, C.R. Thorne, P. Tacconi (Editors), Dynamics of Gravel-Bed Rivers. John Wiley & Sons, Chichester, pp. 55–71.

Bunte, K., Abt S.R., Potyondy, J.P., Ryan, S.E., 2004. Measurement of coarse gravel and cobble transport using portable bedload traps. *Journal of Hydraulic Engineering* 130: 879–893.

Carling, P.A., Williams, J.J., Kelsey A., Glaister M.S., Orr, H.G., 1998. Coarse bedload transport in a mountain river. *Earth Surface Processes and Landforms* 23: 141–157. DOI: 10.1002/(SICI)1096-9837(199802)23:2<141::AID-ESP827>3.0.CO;2-J.

Cudden, J.R., Hoey, T.B., 2003. The causes of bedload pulses in a gravel channel: the implications of bedload grain-size distributions. *Earth Surface Processes and Landforms* 28: 1411–1428.

DOI:10.1002/esp.521.

Dietrich, W.E., Kirchner J.W., Ikeda H., Iseya F., 1989. Sediment supply and the development of the coarse surface layer in gravel-bedded rivers. *Nature* 340: 215–217. DOI:10.1038/340215a0.

Emmett, W.W., 1980. A field calibration of the sediment trapping characteristics of the Helley-Smith bedload sampler. *U. S. Geological Survey Professional Paper*, 1139, 44 pp.

Emmett, W.W., Wolman M.G., 2001. Effective discharge and gravel bed rivers. *Earth Surface Processes and Landforms* 26: 1369–1380. DOI: 10.1002/esp.303.

Ferguson, R.I., 1994. Critical discharge for entrainment of poorly sorted gravel. *Earth Surface Processes and Landforms* 19: 179–186.

Fujita, M., Mizuyama T., Sawada T., Niihara S., 2005. Restoration process of pools filled up with sediment in step-pool bed form. *Journal of the Japan Society of Erosion Control Engineering* 58(3): 25–33 (In Japanese with English abstract).

Garcia, C., Laronne, J., Sala, M., 1999. Variable source areas of bedload in a gravel-bed stream. *Journal of Sediment Research* 69: 39–43.

Garcia, C., Laronne, J., Sala, M., 2000. Continuous monitoring of bedload flux in a mountain gravel-bed river. *Geomorphology* 34: 23–31.

Geertsema, M., Pojar, J.J., 2007. Influence of landslides on biophysical diversity—A perspective from British Columbia. *Geomorphology* 89: 55–69. DOI:10.1016/j.geomorph.2006.07.019.

Gibbins, C., Vericat, D., Batalla, R.J., 2007. When is stream invertebrate drift catastrophic? The role of hydraulics and sediment transport in initiating drift during flood events. *Freshwater Biology* 52: 2369–2384. DOI: 10.1111/j.1365-2427.2007.01858.x.

Gomi, T., Sidle R.C., 2003. Bedload transport in managed steep-gradient head water streams of southern Alaska. *Water Resources Research* 39: 1336. DOI 10.1029/2003WR002440.

Gomi, T., Sidle R.C., Richardson J.S., 2002. Understanding processes and downstream linkages of headwater systems. *BioScience* 52: 905–916.

Gomi, T., Sidle R.C., Swanston, D.N., 2004. Hydrogeomorphic linkages of sediment transport in headwater streams, Maybeso Experimental Forest, southwest Alaska. *Hydrological Processes* 18: 667–683. DOI: 10.1002/hyp.1366.

Hartman, G.F., Scrivener, J.C., Miles M.J., 1996. Impacts of logging in Carnation Creek, a high-energy coastal stream in British Columbia, and their implication for restoring fish habitat. *Canadian Journal of Fisheries and Aquatic Sciences* 53 (Suppl. 1): 237–251.

Imaizumi, F., Sidle R.C., 2007. Linkage of sediment supply and transport processes in Miyagawa Dam catchment, Japan. *Journal of Geophysical Research* 112: F03012. DOI:10.1029/2006JF000495.

Imaizumi, F., Yamamoto, T., Tsuchiya, S., Ohsaka, O., 2005. Characteristics of the bedload and suspended sediment in a small torrent—Evidence from intense field sampling for understanding sediment transport mechanism. *Journal of the Japan Society of Erosion Control Engineering* 57(6): 13–20 (In Japanese with English abstract).

Komar, R.D., Shih S., 1992. Equal mobility versus changing bedload grain sizes in gravel-bed streams. In: P. Billi, R.D. Hey, C.R. Thorne, P. Tacconi (Editors), Dynamics of Gravel-Bed Rivers. John Wiley & Sons, Chichester, pp. 73–105.

Kuhnle, R.A., 1992. Fractional transport rates of bedload on Goodwin Creek. In: P. Billi, R.D. Hey, C.R. Thorne, P. Tacconi (Editors), Dynamics of Gravel-Bed Rivers. John Wiley & Sons, Chichester, pp. 141–155.

Laronne, J.B., Gracia, C., Reid, I., 2001. Mobility of patch sediment in gravel bed streams: patch character and its implications for bedload. In: M.P. Mosley (Editor), Gravel-Bed Rivers V. New Zealand Hydrological Society Inc., New Zealand, pp. 249–389.

Lenzi, M.A., 2001. Step-pool evolution in the Rio Cordon, northeastern Italy. *Earth Surface Processes and Landforms* 26: 991–1008. DOI:10.1002/esp.239.

Lenzi, M.A., D'Agostino V., Billi P., 1999. Bedload transport in the instrumented catchment of the Rio Cordon Part I: Analysis of bedload records, conditions and threshold of bedload entrainment. *Catena* 36: 171–190. DOI:10.1016/S0341-8162(99)00016-8.

Lenzi, M.A., Mao, M., Comiti, F., 2006. When does bedload transport begin in steep boulder-bed streams? *Hydrological Processes* 20: 3517–3533.

Lisle, T.E., Cui, Y., Parker, G, Pizzuto, J.E., Dodd, A.M., 2001. The dominance of dispersion in the evolution of bed material; waves in gravel bed rivers. *Earth Surface Processes and Landforms* 26: 1409–1420. DOI: 10.1002/esp.300.

Lisle, T.E., Hilton, S., 1999. Fine bed material in pools of natural gravel bed channels. *Water Resources Research* 35: 1291–1304.

Miller, D., Luce, C., Benda, L., 2003. Time, space, and periodicity of physical disturbance in streams. *Forest Ecology and Management* 178: 121-140, DOI:10.1016/S0378-1127(03)00057-4

Montgomery, D.R., Buffington, J.M., 1997. Channel-reach morphology in mountain drainage basins. *Geological Society of America Bulletin* 109: 596–611.

Montgomery, D.R., Panfil, M.S., Hayes, S.K., 1999. Channel-bed mobility response to extreme sediment loading at Mount Pinatubo. *Geology* 27: 271–274.

Parker, G., Klingeman, P., McLean, D., 1982. Bedload and size distributions in paved gravel-bed streams. *Journal of the Hydr. Division ASCE* 108 HY4: 544–571.

Rosen, D.L., 1994. A classification of natural rivers. *Catena* 22: 69–199.

Sawada, T., 1985. Sediment transport in mountain basins. Doctoral thesis, Kyoto University.

Sidle, R.C., 1998. Bedload transport regime of a small forest stream. *Water Resources Research* 24: 207_218.

Vericat, D., Church, M., Batalla, R.J., 2006. Bedload bias: Comparison of measurements obtained using two (76 and 152 mm) Helley-Smith samplers in a gravel bed river. *Water Resources Research* 42: W01402.

Wilcock, P.R., 1992. Experimental investigation of the effect of mixture properties on transport dynamics, In: P. Billi, R.D. Hey, C.R. Thorne, P. Tacconi (Editors), Dynamics of Gravel-Bed Rivers. John Wiley & Sons, Chichester, pp. 73–105.

Wilcock, P.R., 1997. The components of fractional transport rate. *Water Resources Research* 33: 247–258.

Wilcock, P.R., McArdell, B.W., 1993. Surface-based fractional transport rates: mobility thresholds and partial transport of a sand-gravel sediment. *Water Resources Research* 29: 1297–1312.

Yano, K., Tsuchiya, Y., Okumura, T., 1967. Some observations on the sediment yield and transport in a mountain watershed. *Annals of Disaster Prevention Research Institute*, *Kyoto University* 10B: 81–96.

Figure captions

Fig 1. Topographic map of Hirudani experimental watershed. Photographs of the dam and bed-load sampling sites are also shown.

Fig 2. Longitudinal profile of the observation sites. The observation sites for water discharge (H_2) and bed-load rate (A and B) are indicated. The distribution of bed forms in the area between sites A and B is shown.

Fig 3. Changes in bed-load rate at sites A and B after opening of the gate of the experimental dam. Discharge, flow velocity and shear stress at sites A and B are also illustrated. Note that the scales differed for the total bed-load rate and the bed-load rate for each size fraction (y-axis).

Fig 4. Grain-size distributions of bed-surface sediment at site H_2 collected before and after the experiment. The size distributions of sediment in the pond of the dam are also presented.

Fig 5. Fractional transport rate soon after opening of the check dam gate (at 11:04 and 11:05 for sites A and B, respectively) and during the passage of the sediment wave (at 12:23 and 12:40 for sites A and B, respectively).

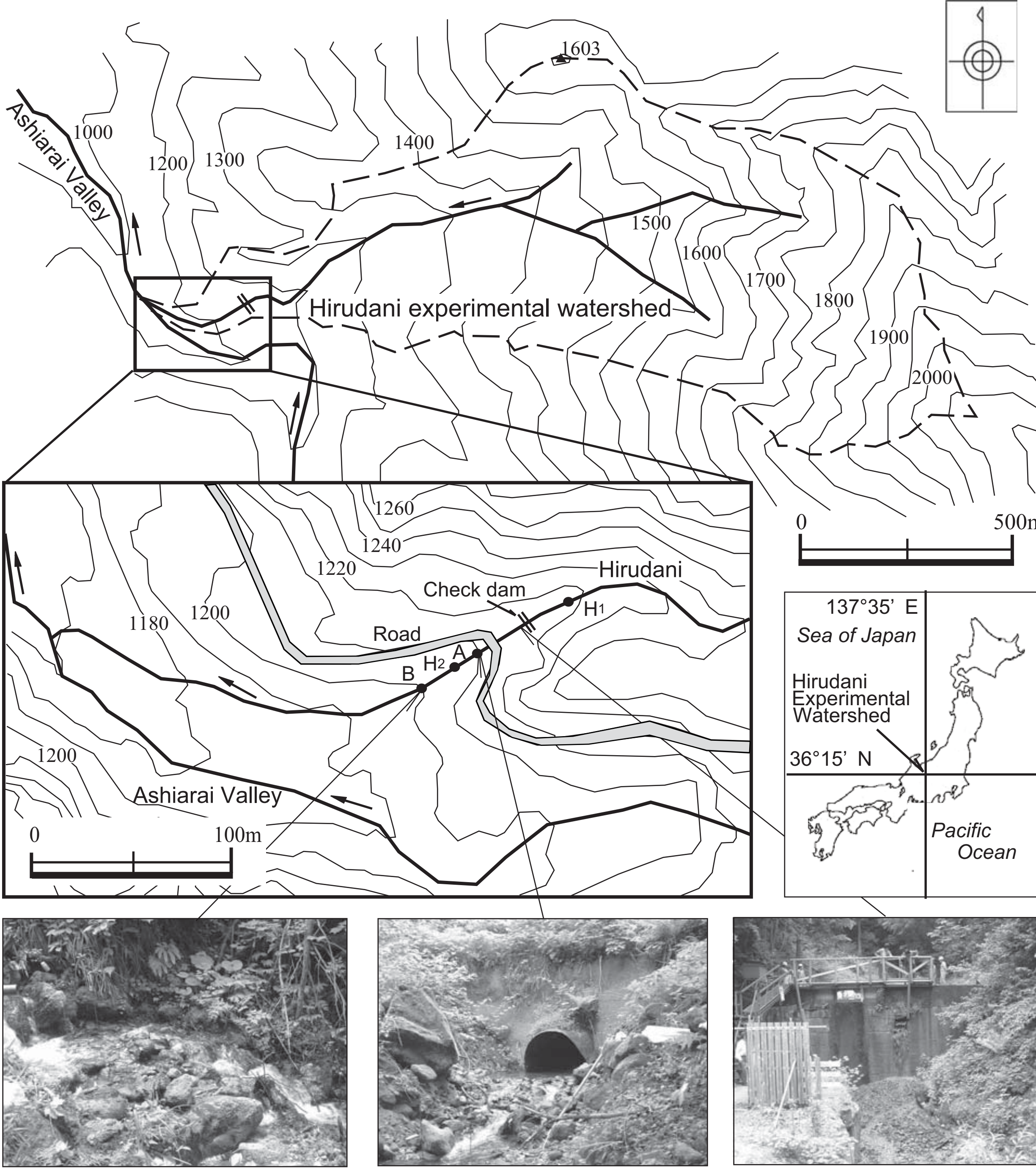
1603
Ashiarai Valley
1000
1200
1300
1400
1500
1600
1700
1800
1900
2000
Hirudani experimental watershed
0
500m
1260
1240
1220
Hirudani
Check dam
H1
Road
A
H2
B
1180
1200
1200
Ashiarai Valley
0
100m
137°35' E
Sea of Japan
Hirudani
Experimental
Watershed
36°15' N
Pacific
Ocean

Figure 1

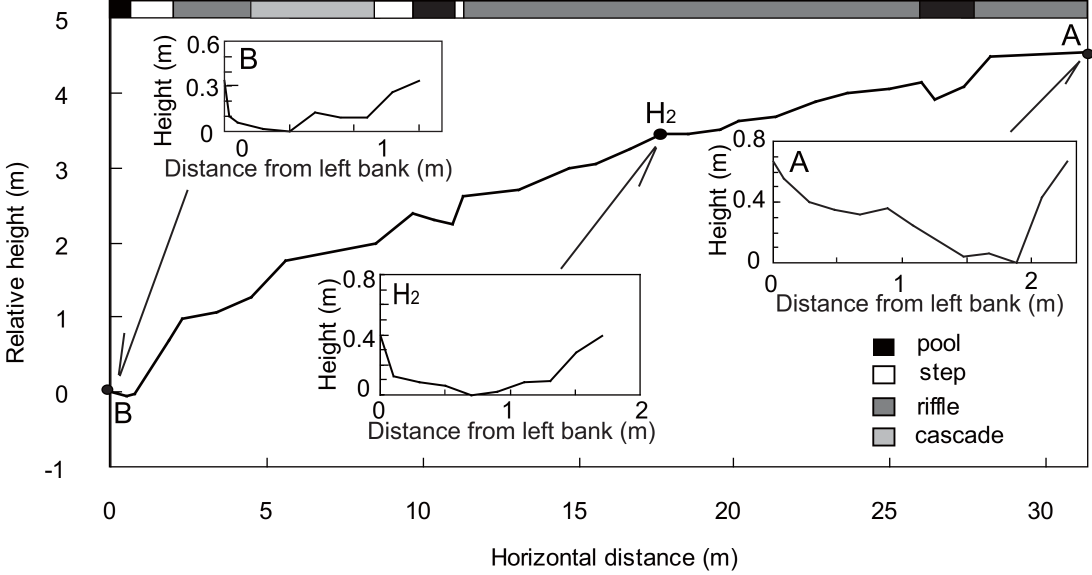

Relative height (m)
Horizontal distance (m)
A
B
H_2
Height (m)
Distance from left bank (m)
pool
step
riffle
cascade

Figure 2

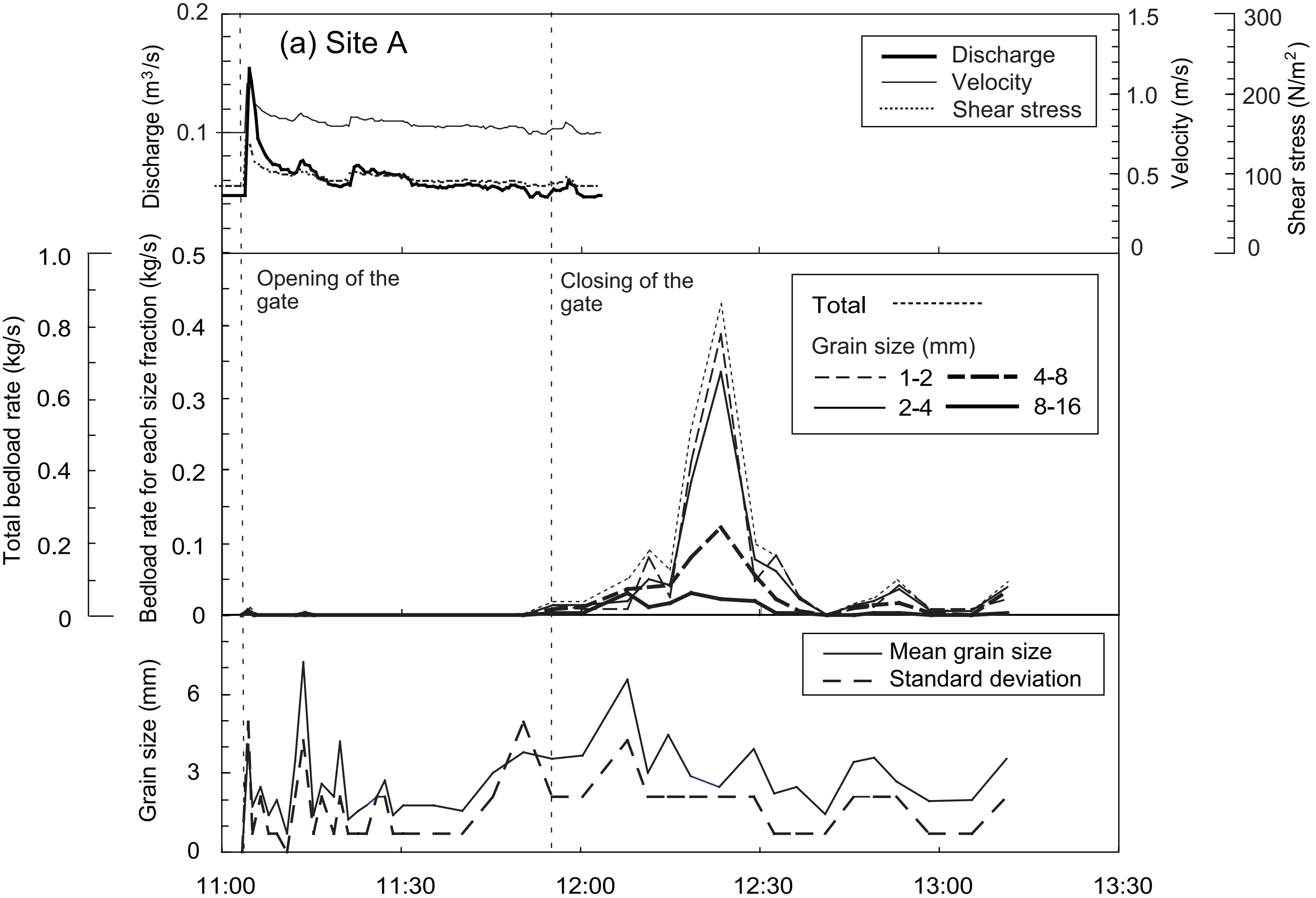

(a) Site A
Discharge
Velocity
Shear stress
Discharge (m3/s)
Velocity (m/s)
Shear stress (N/m2)
Opening of the gate
Closing of the gate
Total
Grain size (mm)
1-2
4-8
2-4
8-16
Total bedload rate (kg/s)
Bedload rate for each size fraction (kg/s)
Mean grain size
Standard deviation
Grain size (mm)
11:00
11:30
12:00
12:30
13:00
13:30

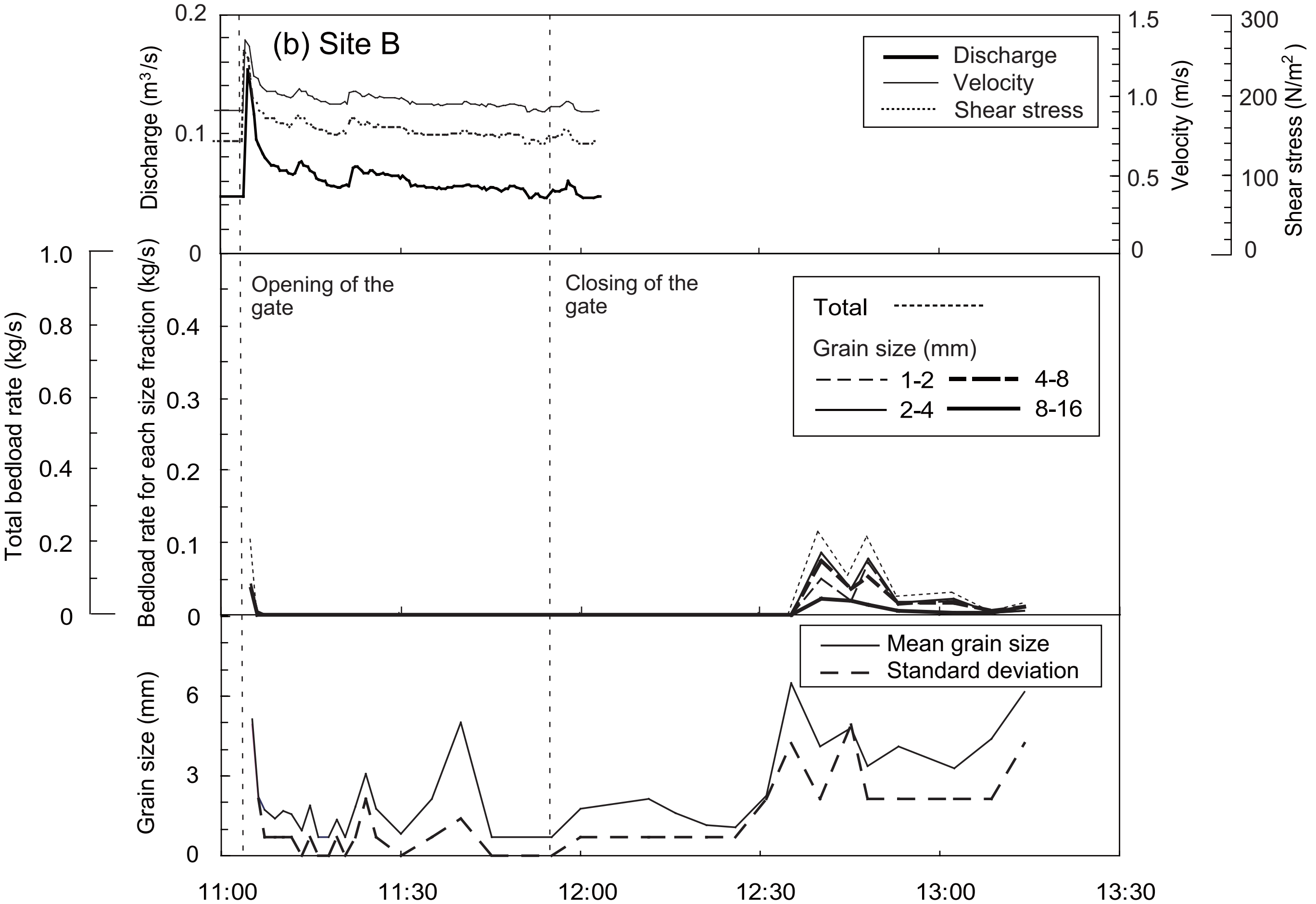

(b) Site B
Discharge
Velocity
Shear stress
Discharge (m3/s)
Velocity (m/s)
Shear stress (N/m2)
Opening of the gate
Closing of the gate
Total
Grain size (mm)
1-2
4-8
2-4
8-16
Total bedload rate (kg/s)
Bedload rate for each size fraction (kg/s)
Mean grain size
Standard deviation
Grain size (mm)
11:00
11:30
12:00
12:30
13:00
13:30

Figure 3

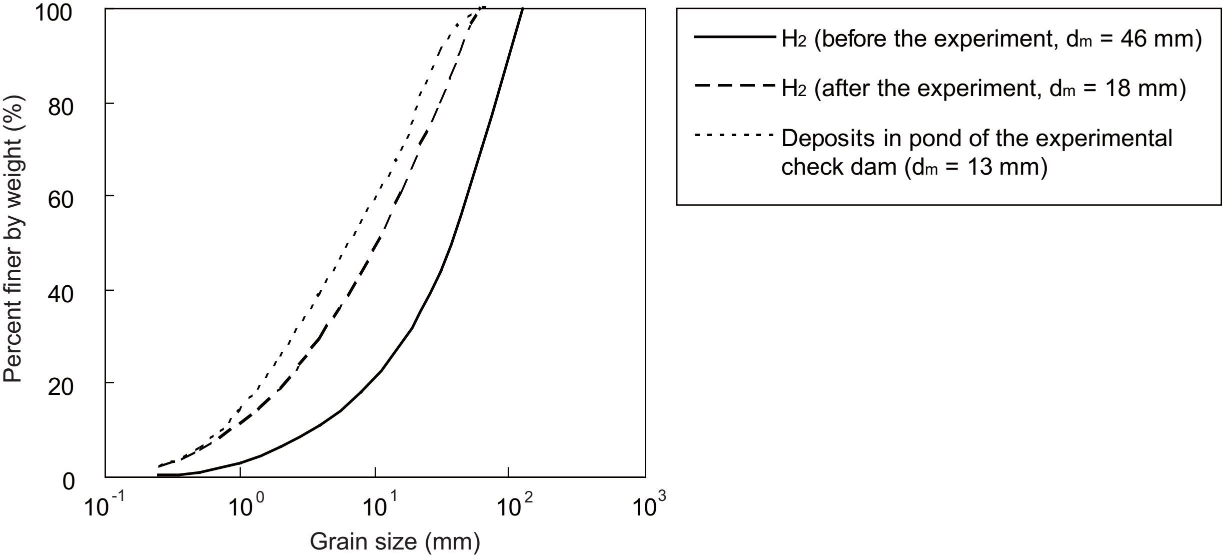

100
80
60
40
20
0
Percent finer by weight (%)
10^{-1}
10^{0}
10^{1}
10^{2}
10^{3}
Grain size (mm)
H2 (before the experiment, dm = 46 mm)
H2 (after the experiment, dm = 18 mm)
Deposits in pond of the experimental check dam (dm = 13 mm)

Figure 4

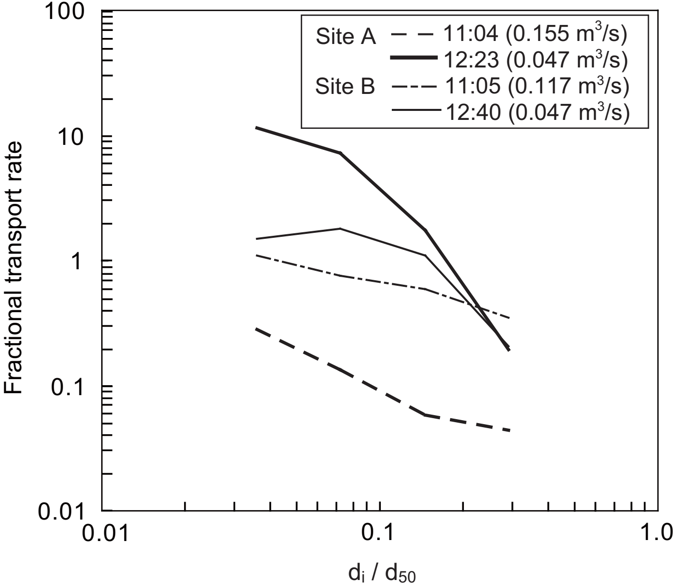

100
10
1
0.1
0.01
0.01
0.1
1.0
Fractional transport rate
d$_i$ / d$_{50}$
Site A
11:04 (0.155 m^3/s)
12:23 (0.047 m^3/s)
Site B
11:05 (0.117 m^3/s)
12:40 (0.047 m^3/s)

Figure 5